

Numerical Simulation of NbTi Superconducting Joint with Cold-Pressing Welding Technology

Feng Zhou, Junsheng Cheng, Jianhua Liu, Yinming Dai, Qiuliang Wang, Namin Xiao, Luguang Yan

Institute of Electrical Engineering, Chinese Academy of Sciences, Beijing, 100190, China
e-mail: zhoufeng@mail.iese.ac.cn

Abstract - The cold pressing welding methods are employed to fabricate joints between NbTi multi-filamentary conductors, and a series of joints are made at the different press amounts for NMR magnet applications. The Abaqus-Explicit method was used to do a quasi-static analysis of the cold-pressing welding process. In the simulation, we consider the contact area and equivalent plastic strain to determine the resistance of the superconducting joints, qualitatively. The simulation shows that a press amount of 61%-65.5% should be the optimum range, in which, the lowest joint resistance can be obtained. Resistances of these joints are also tested using the current decay method to verify the simulation.

Submitted September 30, 2013, accepted October 12, 2013. Reference No. ST347; Category 5.
Final version of this paper was published in IEEE Trans. Appl. Supercond. **23**, 4802706 (2013); DOI:
[10.1109/TASC.2013.2277779](https://doi.org/10.1109/TASC.2013.2277779)

Keywords - NbTi superconducting joint; cold-pressing welding; resistance; Abaqus-Explicit methods.

I. INTRODUCTION

NbTi joints are inevitable in the superconducting magnet for NMR applications due to the limitation of wire length. They are always used to connect two adjacent coils. The persistent current of an NMR magnet is very important, which is dependent upon the resistive losses within the coil circuit [1]. The total resistance in the magnet system comes from superconducting wire resistance and joint resistance [2, 3]. Because the wire resistance can be decreased by increasing the current margin during design, the joints between coils and switches must be fabricated carefully to achieve high magnetic field stability in the NMR system [4].

The joints between NbTi multi-filamentary conductors can be fabricated by many methods, such as, solder welding [5], cold-pressing welding [6,7] and dip welding, diffusion bonding [8], electromagnetic forming [9] and solder matrix replacement. Among these methods, the cold-pressing welding method is well suited to fabricate NbTi superconducting joints because of its reliability.

In this paper, we used the software Abaqus-Explicit method to simulate a quasi-static analysis of the cold-pressing welding process for NbTi superconducting joints. In the simulation, we mainly considered two factors, *i.e.*, contact area and equivalent plastic strain, to determine the resistance of NbTi joint qualitatively. Resistance testing results were also discussed to verify the conclusion to obtain from the simulation. The purpose of this research is to find the optimum press amount in the NbTi superconducting joint cold-pressing welding process.

II. FABRICATION OF JOINTS

The NbTi/Cu wire used to fabricate the joints is F54 supplied by Oxford Instruments, which has a bare diameter of 0.4 mm, and a Cu/non-Cu ratio of 1.35. The NbTi/Cu tube has a length of 3 cm, external diameter of 4 mm, and internal diameter of 2 mm; the configuration of the cross-section of NbTi/Cu tube is shown in Figure 1. The cold-pressing welding process includes the following steps:

- (I). Remove the insulation layer on wire by abrasive paper.
- (II). Remove the stabilizer on the wire by nitric acid until the filaments appear.
- (III). Clean the filaments by pure water and ethanol.
- (IV). Dry the filaments in open air.
- (V). Install the filaments in a NbTi/Cu tube.
- (VI). Press the NbTi/Cu tube in open air.

The six NbTi superconducting joints are fabricated with the different press amounts. The press amount is defined as:

$$p = \frac{\Delta d}{D} \times 100\% \quad (1)$$

where Δd is the press displacement, D is the external diameter of NbTi/Cu tube. The press amounts used in this simulation are: 49.5%, 54%, 61%, 65.5%, 69.5%, 70.5%. The samples before and after the press operation are shown in Figure 2.

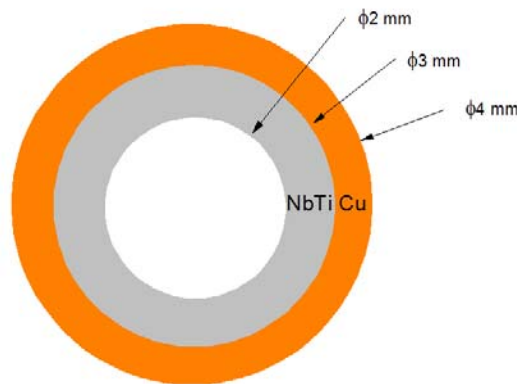


Fig. 1. Schematic cross-section of NbTi/Cu tube.

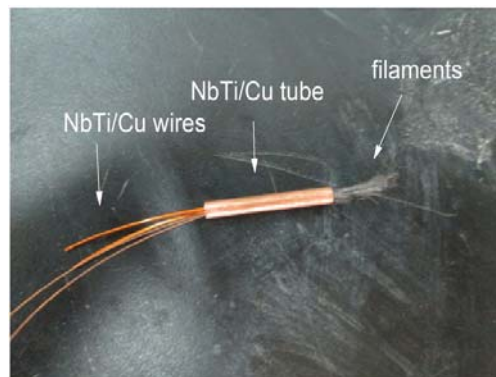


Fig. 2 (a). NbTi joint samples, before press operation.



(b)

Fig. 2 (b). NbTi joint samples, (a) before press operation, after press operation.

III. SIMULATION

A. Analytical Model

A three dimension (3D) finite element (FE) model of the NbTi cold-pressing welding joint was constructed using Abaqus-Explicit. Figure 3 shows parameters of the analytical model. To simplify the model, the Cu layer was ignored, and the external diameter of tube model turns 3 mm. Since NbTi is much harder than Cu, this ignorance will not influence the result seriously. The distribution of filaments is shown in Fig.3(b). A fully fixed boundary condition was applied on the die, and displacement boundary condition was applied on the punch. Contact exists between tube and filaments, and among filaments. A general contact was applied to model the complex contact behavior in the process. A Coulomb friction model was used here. We did an NbTi friction experiment to get the friction coefficient equaling 0.72. 8-noded solid elements (C3D8R) were used for the simulation with 9 element layers through the tube thickness and 20 element layers through the tube length.

The input to the model consists of NbTi elastic properties and plastic properties. An elastic-plastic tensile experiment of NbTi was carried out. The result of true stress and logarithmic strain is shown in Fig. 4. From Figure 4 we get: (a) elastic modulus is 60.5 Gpa; (b) NbTi yields at $\varepsilon = 1.2\%$; (c) NbTi begins to damage at equivalent plastic strain $\varepsilon_0^{pl} = 11\%$. Since the stress-strain relationship no longer represents the material's behavior accurately when material necking occurs, an ideal plastic pattern (BC in Fig. 4.) is applied in place of the softening branch (BD in Fig. 4.) [10]. Poisson ratio, 0.33, is cited from [11]. The density of NbTi, 6027 kg/m³, can be calculated from the proportion of components Nb 47wt.% Ti.

B. Load

A displacement boundary condition was applied on the punch to press the tube in the model. It is not necessary to define the analysis time as the actual time, since that will make the calculation time too long. We did a quasi-static analysis and defined the analysis time as 0.25 ms to speed up the simulation process. So the punching speed is ~15 m/s in model. The press displacement of punch is applied in a smooth step. Table I shows the maximum kinetic energy (KE) and the corresponding internal energy (IE) in the press process of six models. From the ratio KE/IE, we can see that six ratios are all less than 10% (typical threshold) [10].

Hence, according to the energy balance principle, the influence of inertia can be ignored [10], and the analysis time of 0.25 ms is appropriate.

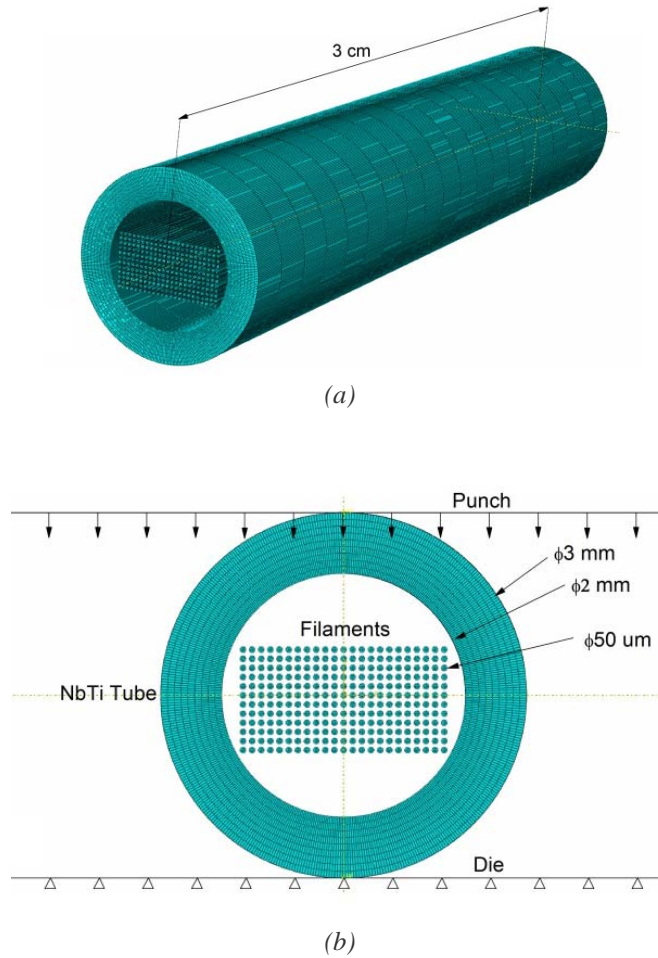


Fig.3. Parameters of the analytical model, (a) the 3D view, (b) the cross-section.

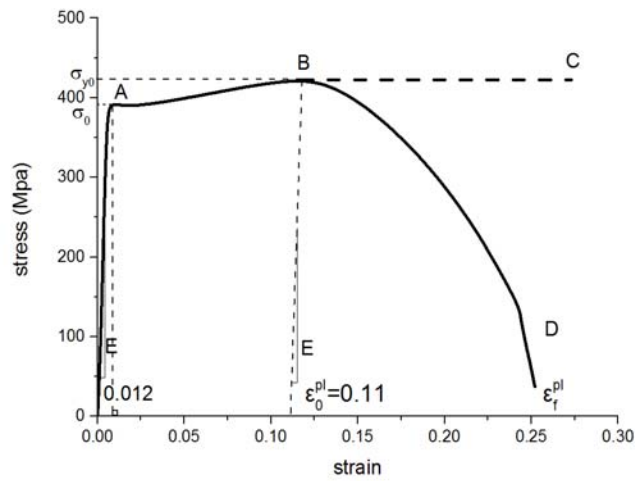


Fig.4. Stress-strain response curve of NbTi superconductor.

TABLE I

Maximum kinetic energy, corresponding internal energy and ratio KE/IE of six models

Model	Max KE(J)	Corresponding IE(J)	$\frac{KE}{IE}$
49.5%	0.311	10.316	3.01%
54%	0.378	12.429	3.04%
61%	0.517	14.457	3.58%
65.5%	0.615	15.196	4.05%
69.5%	0.701	15.697	4.47%
70.5%	0.726	16.726	4.34%

C. Simulation Results and Discussions

Six models with different press amounts with 49.5%, 54%, 61%, 65.5%, 69.5%, 70.5% were simulated. We mainly consider filaments' contact area and equivalent plastic strain to determine the joint's resistance qualitatively. Since increasing contact is in favor of decreasing joint resistance but increasing strain damage is against that, the lowest joint resistance must be obtained when contact is good and strain damage is small at the same time. However, as the press amount increases, contact area and strain damage will both increase. So there must be an equilibrium point.

The definition of the contact area among filament is shown in Figure 5 (the red region). Figure 6 shows the model cross-section after press operation and equivalent plastic strain distribution of filaments of 49.5%, and Figures 7 and 8 shows that of 61% and 70.5%, respectively. For the cases with press amount of 49.5% and 54%, their cross-sections show that there are large voids in the joint, the filaments do not contact well; and equivalent plastic strain distribution shows that very few filaments' equivalent plastic strain exceeds 11% to damage. For 61% and 65.5%, the cross-section shows that there are few voids in the joint, the filaments contact well; and equivalent plastic strain distribution shows that strain is concentrated in the middle section relative to the edges; the equivalent plastic strain of filaments on the edges is less than 11%. For 69.5% and 70.5%, the cross-section shows that there are no voids in the joint, the filaments contact very well; but equivalent plastic strain distribution shows that almost all the equivalent plastic strain of the superconducting filaments severely exceeds 11% to damage or even fracture. According to our assumptions mentioned above, we qualitatively consider the press amount 61%-65.5% should be the optimum range, in which, the lowest joint resistance can be obtained.

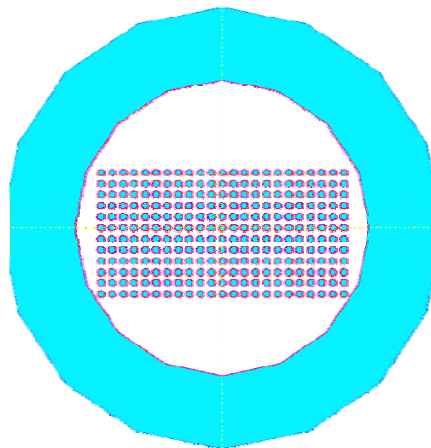
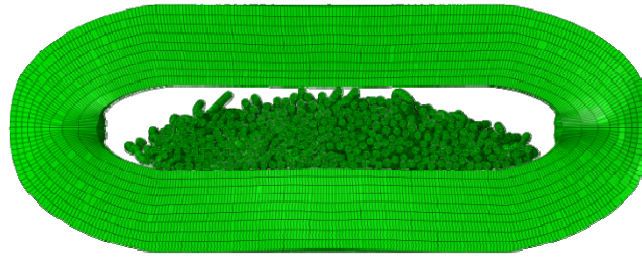
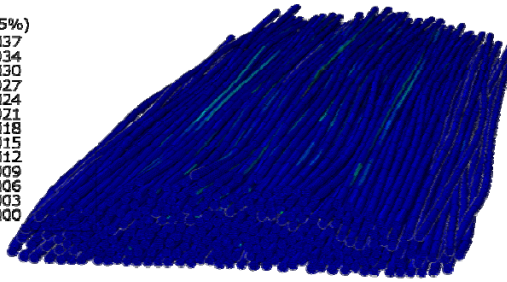
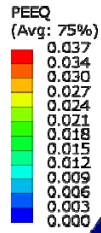


Fig.5. The definition of contact area (the red region).

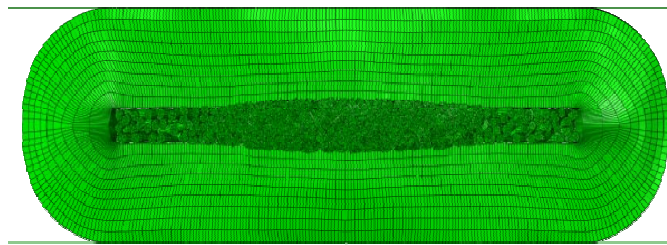


(a)

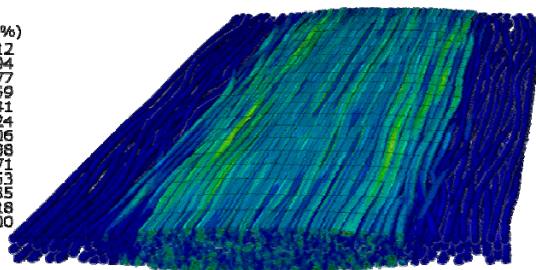
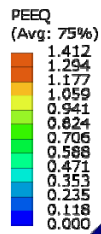


(b)

Fig.6. After press operation, (a) the model cross-section, (b) filaments' equivalent plastic strain distribution for the case with press amount of 49.5%.



(a)



(b)

Fig.7 After press operation, (a) the model cross-section, (b) filaments' equivalent plastic strain distribution for the case with press amount of 61%.

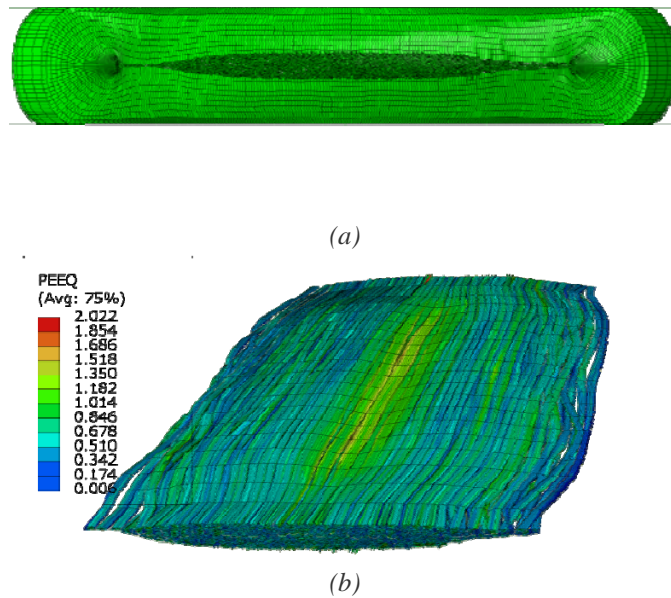


Fig.8. After press operation, (a) the model cross-section, (b) filaments' equivalent plastic strain distribution for the case with press amount of 70.5%.

Figure 9 shows the contact area of six models after press operation. Figure 10 shows the average value of equivalent plastic strain of the six models' filaments after press operation. From Figures 9 and 10 we can see that as press amount increases, the contact area and average equivalent plastic strain will both increase. However, their increasing trends are different. The contact area increases slowly at first; then after 54%, it increases very fast; but after 61%, it begins to increase slowly again to reach a stable value; while the average equivalent plastic strain increases slowly at first similarly, but after 54% it can be considered to increase in an approximately linear form. The value of contact area and equivalent plastic strain can be used in further research based on the equation:

$$R = f(S, \epsilon^{pl}) \tag{2}$$

where R is the joint resistance, S and ϵ^{pl} are the contact area and equivalent plastic strain, respectively. The equation can be used to calculate the theoretical joint resistance value quantitatively and we are still working on this.

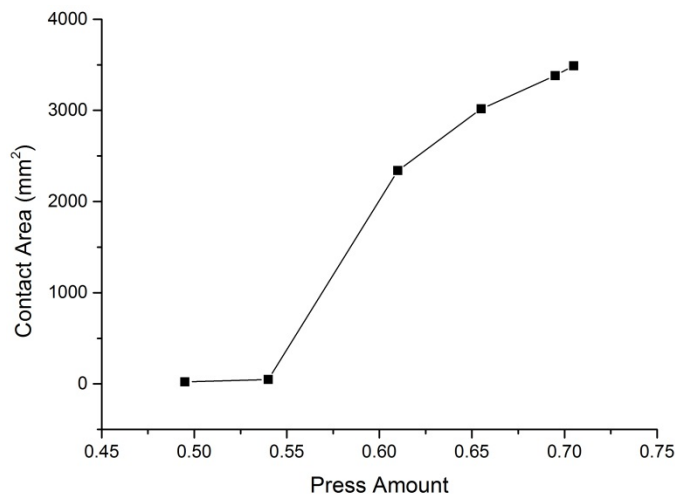


Fig.9. Contact area of six models after press operation.

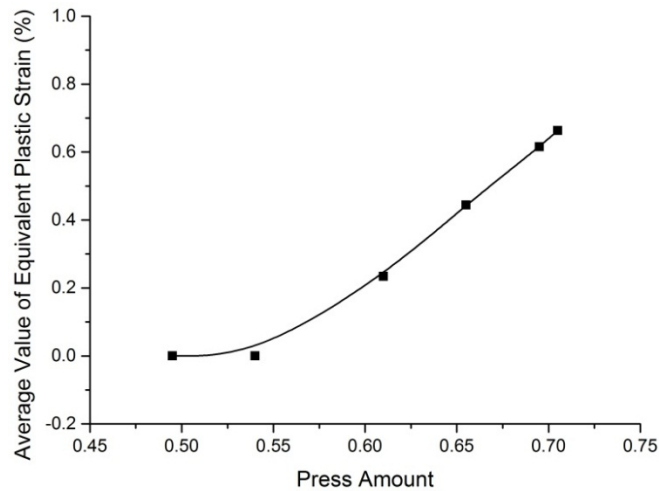


Fig.10. Average value of equivalent plastic strain of six models' filaments after press operation.

IV. EXPERIMENT

Resistances of the six samples in 0-1 T background magnetic field were tested using the current decay method to verify the conclusion we got from simulation. Figure 11 shows the results. We also used a scanning electron microscope (SEM) to observe cross-sections of these samples, shown in Figure 12.

Figure 11 shows that the joint resistance increases with increasing background magnetic field; the joint resistances of 61% and 65.5% are smaller than the other samples, which correspond with the conclusion from the simulation.

Figure 12 (a) shows the cross section of the filaments after 49.5% press amount, there are some obvious voids; the filaments do not contact well; the deformation of filaments is small. Fig.12 (b) shows the cross section of the filaments after 61% press amount, there are no obvious voids; the filaments contact well; the deformation of filaments is moderate. Figure 12(c) shows the cross section of the filaments after 70.5% press amount, there are no voids; the filaments contact more tightly; the deformation of filaments is severe. These experimental results are indicated in Figures 6, 7 and 8.

As shown in Table II, the resistance testing results and cross-sections under SEM of six samples demonstrate that the joint resistance's relationship with contact area and strain damage is as we predict. Our assumption of considering contact area and equivalent plastic strain to determine the joint's resistance qualitatively is appropriate.

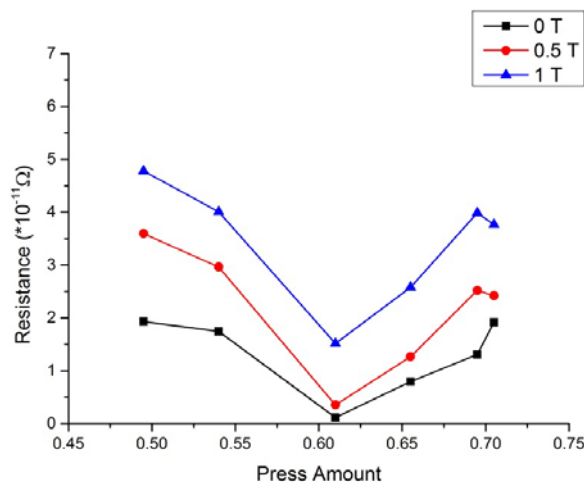
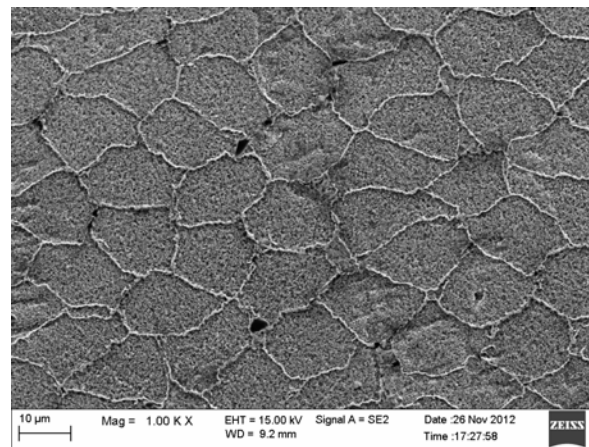
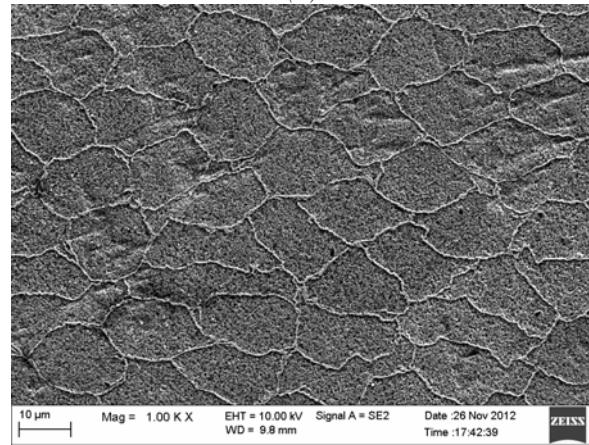


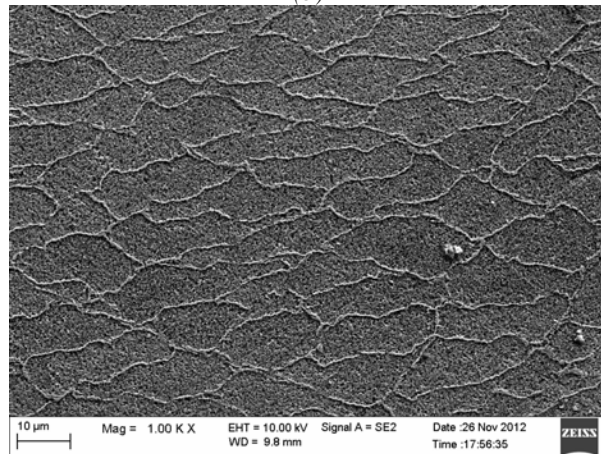
Fig.11. Resistances of six samples in 0-1 T background magnetic field.



(a)



(b)



(c)

Fig.12. Cross-sections of joints with different press amounts, (a) 49.5%, (b) 61%, (c) 70.5%.

TABLE II

Joint resistance's relationship with contact area and strain damage from experiment

Samples	Joint Resistance	Contact	Deformation
49.5%-54%	Relatively high	Not good	Small
61%-65.5%	Relatively Low	Good	Moderate
69.5%-70.5%	Relatively high	Very good	Severe

V. CONCLUSIONS

Six NbTi cold-pressing welding superconducting joints were made at different press amounts for NMR application. This research used Abaqus-Explicit to do a quasi-static analysis of the cold-pressing welding process for these joints. In the simulation, two factors – contact area and equivalent plastic strain – were mainly considered to determine the joint's resistance qualitatively. The simulation showed that a press amount of 61%-65.5% should be the optimum range. To verify the conclusion from our simulation, resistances of six samples in 0-1 T background magnetic field were tested by the current decay method and cross-sections of these joints were observed by SEM. The experimental results agree well with the simulation ones. Further research on the equation $R = f(S, \varepsilon^{Pl})$ will be carried out to calculate the theoretical joint resistance quantitatively.

ACKNOWLEDGEMENT

This work was supported by the National Natural Science Foundation of China under Grants 50925726 and 10755001 and by the Instrument Program in MOST.

REFERENCES

- [1] Qiuliang Wang, "High field superconducting magnet: Science, Technology and Applications," *Progress in Physics* **33**, no.1, 1-23 (2013).
- [2] C.A. Swenson and W.D. Markiewicz, "Persistent joint development for high field NMR," *IEEE Trans. Appl. Supercond.* **9**, no.2, 185-188 (1999).
- [3] Qiuliang Wang, *Practical Design of Magnetostatic Structure using Numerical Methods*, Wiley, 2013, USA.
- [4] P. McIntyre, Y. Wu, G. Liang, and C.R. Meitzler, "Study of Nb₃Sn superconducting joints for very high magnetic field NMR spectrometers," *IEEE Trans. Appl. Supercond.* **5**, no.2, 238-241 (Jun. 1995).
- [5] K.Seo, S. Nishijima, K. Katagiri, and T. Okada, "Evaluation of solders for superconducting magnetic shield," *IEEE Trans. Magn.* **27**, no.2, 1877-1880, (1991).
- [6] Q. Wang, X. Hu, S. Song, L. Ding, L. Yan, A method for the lower resistance superconducting joints with magnetic field shielded, Chinese Patent ZL 201010123276.0
- [7] Junsheng Cheng, Jianhua Liu, Zhipeng Ni, *et al.*; "Fabrication of NbTi Superconducting Joints for 400-MHz NMR Application", *IEEE Trans. Appl. Supercond.* **22**, No. 2, 4300205 (2012).
- [8] H.M. Wen, L.Z.Lin, and S. Han, "Joint resistance measurement using current-comparator for superconducting wires in high magnetic field," *IEEE Trans. Magn.* **28**, No.1, 834-836 (1992).
- [9] Q. Wang, X. Hu, J.Cheng, L.yan, H. Wang, C.Cui, Electromagnetic Forming for Superconducting Joints, Chinese Patent 201210278270.X.
- [10] Dassault, *Abaqus Analysis User's Manual, Abaqus 6.11*, Champs Elysees, France, 2011.
- [11] Wei Qinwei, Hu Jishi, Dong Liang, *et al.*, "Electromagnetic-structural Coupling Analysis of the Pulse Superconducting Magnet Based on ANSYS," (In Chinese), *Science Technology and Engineering*, no.15, 4395-4397 (2009).